*International Journal of Bioelectromagnetism* *www.ijbem.org*
Vol. 12, No. 4, pp. 177 - 182, 2010

# Framework for Continuous Quantification of Spectral Coherence using Quadratic Time-Frequency Distributions: Exploring Cardiovascular Coupling

**Michele Orini[abc], Raquel Bailón[ab], Eduardo Gil[ab], Luca T Mainardi[c], Pablo Laguna[ab]**

[a]*GTC, Aragón Institute of Engineering Research, University of Zaragoza, Zaragoza, Spain*
[b]*CIBER de Bioingenieria, Biomateriales y Nanomedicina, CIBER-BBN, Zaragoza, Spain*
[c]*Department of Biomedical Engineering, Politecnico di Milano, Italy*

Correspondence: M Orini, University of Zaragoza, c/ Maria de Luna 1, 50018, Zaragoza, Spain. E-mail: mihchele@unizar.es

***Abstract.*** Quadratic time-frequency (TF) distributions have an excellent joint TF resolution, but their applicability is limited by the presence of interferences. Interferences make a measure of TF coherence (TFC) based on these distributions inconsistent, unless a specific methodology is used to reduce their influence. In this study, a framework for robustly estimating TFC, based on signal-dependent smoothing of the Wigner Ville distribution, is shown to provide a reliable continuous quantification of cardiorespiratory and cardiovascular interactions during non stationary conditions. Performance of the estimator is evaluated through a simulation example. Linear coupling between heart rate variability and pulse transit time variability is then explored during segments of polysomnography recordings characterized by decreases in the amplitude fluctuations of photopletysmography related to obstructive sleep apnea. It is observed that when a sympathetic activation, related to a decrease in the amplitude fluctuations of photopletysmography, occurs TFC increases in low frequency [0.04,0.15 Hz] range and decreases in high frequency [0.15, 0.4 Hz] range ($p < 0.05$).

*Keywords: Time-frequency analysis, spectral coherence, heart rate, pulse transit time, cardiovascular interactions, obstructive sleep apnea*

## 1. Introduction

Spectral coherence has been widely applied to quantify the strength of linear relationship between two signals. This measure, being defined in the frequency domain, can not assess the time evolution of the coupling between two signals and it is not appropriate to study non stationary signals or transient phenomena. To assess the time evolution of linear coupling an extension of spectral coherence in time-frequency (TF) domain is necessary. In literature, multivariate parametric analysis has been proposed to continuously measure the mutual interaction between heart rate variability (HRV) and systolic blood pressure variability during tilting [Mainardi and al, 1997]. Another model based time-varying coherence function, able to estimate separately feedforward and feedback path of a close-loop, has been recently proposed and applied to explore the coupling of renal blood pressure and blood flow [Zhao et al.,2007]. Parametric models are attractive because, thanks to their mathematical modelling, they provide a way to disentangle feedback and feedforward mechanisms, to identify systems also in close-loop conditions [Porta et al.,2006] and to evaluate the causal direction of a coupling [Porta et al.,2002]. Nevertheless, their performance in estimating the time varying spectral characteristics of a signal is related to the capability of fitting the appropriate underlying model and, in extremely non stationary conditions, they have been observed to perform less accurately than non parametric methods [Orini et al.,2007]. In a non parametric context, a measure of time-scale coherence, based on Continuous Wavelet Transform, has been recently applied to the study of cardio-respiratory interactions [Keissar et al.,2009]. Non parametric methods have the advantage that they do not need any kind of assumption on the mathematical structure of the observed phenomenon and that they are relatively easy to estimate. Quadratic TF distributions represent a very powerful tool for the study of non stationary signals and transient phenomena and they have been widely applied to the study of autonomic nervous modulation [Mainardi et al.,2009]. Theoretical properties of TF coherence $\gamma(t,f)$ defined using quadratic distributions have been first described in [White et al.,1990] and [Matz and Hlawatsch,2000], but, to our knowledge, it has never been used in biomedical applications. Quadratic TF coherence is defined as:

$$\gamma^2(t,f) = \frac{C_{xy}(t,f)C_{xy}^{*}(t,f)}{C_x(t,f)C_y(t,f)} \tag{1}$$

where $C_{xy}(t,f)$ is the cross TF spectrum and $C_x(t,f)$ and $C_y(t,f)$ are the auto TF spectra, of signals $x(t)$ and $y(t)$, respectively. In [White et al.,1990] authors claim that choosing the positive distributions of the Cohen's class, the TFC in (1) maintains the desirable properties of the spectral coherence, in particular, it results to be bounded almost surely by unity (0 for totally uncorrelated signals and 1 for perfect linear correlation). In [Matz and Hlawatsch,2000] it has been shown how (1) is properly bounded for jointly *underspread* processes, i.e. processes $x(t)$ and $y(t)$ should not have a widespread TF correlation. The main problem for the definition of a TFC based on quadratic distributions and bounded by unity is related to the presence of interference terms (ITs). Biological signals are often highly correlated in time and frequency (overspread) and a smoothing is needed to suppress ITs, but at detriment of joint TF resolution. The main purpose of this study is to present a robust estimator for TF coherence, which should range between 0 and 1 at least in specific TF regions of interest, based on signal-dependent quadratic TF representations. Its suitability for the continuous estimation of the interactions in cardiorespiratory and cardiovascular systems during non stationary conditions is discussed through a simulation study. Real data application aiming at exploring the linear relationship between HRV and pulse transit time variability (PTTV) will be also presented. The high frequency component (HF, range [0.15-0.4] Hz) of the HRV signal is known to be strictly related to the parasympathetic system, through respiratory sinus arrhythmia (RSA), while the low frequency component (LF,range [0.04-0.15] Hz) of the PTTV signal is thought to be directly affected by sympathetic vasoconstriction. The other two components (LF of HRV and HF of PTTV) are not that clearly related to an unique phenomenon. The quantification of the linear coupling between HRV and PTTV spectral components during decrease in the amplitude fluctuations of photopletysmography (DAP), may provide useful information for better understanding how autonomic modulation is reflected in both signals.

## 2. Methods

### 2.1. Smoothed pseudo Wigner-Ville distribution

The Wigner Ville distribution (WVD) is known to provide an excellent joint TF resolution. Unfortunately, the presence of ITs makes its applicability very limited. In order to reduce ITs, smoothed versions of the WVD, belonging to the Cohen's Class, have been proposed. Smoothing is performed as a 2D convolution between the WVD and a 2D kernel (defined in TF plane), which completely defines the properties of the distribution. Each distribution in the Cohen's Class can be interpreted as the 2D Fourier transform of a weighted version of the Ambiguity Function (AF) of the signal to be analyzed [Hlawatsch and Flandrin,1991]. The cross-TF spectrum can be defined as:

$$\begin{aligned} C_{xy}(t,f;\varphi) &= W_{xy}(t,f) ** \varphi(t,f) = \underset{\nu\to t,\tau\to f}{FT}\{A(\nu,\tau)\Phi(\nu,\tau)\} \\ A_{xy}(\nu,\tau) &= \underset{t\to\nu}{FT}\{x(t+\tau/2)x^{*}(t-\tau/2)\} \\ \Phi(\nu,\tau) &= \underset{t\to\nu,\, f\to\tau}{FT}\{\varphi(t,f)\} \end{aligned} \tag{2}$$

In (2) $**$ is the 2D convolution on $t$ and $f$, $FT$ is the Fourier Transform operator and $A_{xy}(\nu, \tau)$ is the cross-AF of signals $x(t)$ and $y(t)$. The weighting (smoothing) function $\Phi(\nu, \tau)$ $(\varphi(t,f))$ performs as a 2D low pass filter which should be tuned in order to find the better trade-off between ITs suppression and joint TF resolution (in TF domain) or, dually, between cross-component suppression and auto-terms concentration (in ambiguity domain). As the geometry of the kernel completely defines the performance of the TF distribution some efforts should be done toward the definition of versatile kernels, capable of automatically adjust to the TF structure of the signals being analyzed [Baraniuk and Jones,1993], [Costa and Bourdeau_Bartles,1995]. Here, an elliptical exponential kernel is used:

$$\Phi(\nu,\tau;\nu_0,\tau_0,\lambda) = \exp\{-\pi[(\nu/\nu_0)^2 + (\tau/\tau_0)^2]^{2\lambda}\} \tag{3}$$

The kernel's iso-contours are ellipsis, $\nu_0$ and $\tau_0$ affect the length of the axes (the bandwidth of the 2D low pass filter) whereas λ sets its roll-off.

### 2.1. The signal-dependent smoothing

Signals affected by the autonomic modulation may be modelled as the sum of complex exponentials showing both amplitude (AM) and frequency (FM) modulation, embedded in noise. In this study two exponentials are considered to model an AM LF and an AM-FM HF component:

$$x(t) = A_{LF}(t)e^{i\theta_{LF}(t)}A_{HF}(t)e^{i\theta_{HF}(t)} + z(t) \qquad (4)$$

where instantaneous frequency is $F(t)=(d\theta(t)/dt)/2\pi$.

Quadratic TF distributions of these kinds of signals are expected to present both outer and inner ITs [Hlawatsch,1997]. In order to suppress outer ITs, which mainly oscillate in time direction with a frequency which locally depends on the frequency lag $\nu_i=F_{HF}-F_{LF}$, the kernel should be able to filter out all $\nu > \nu_{i,min}$, where $\nu_{i,min}$ corresponds to the slowest ITs. To obtain $\nu_{i,min}$, the estimation of $F_{LF}(t)$ and $F_{HF}(t)$ is required. A direct or indirect estimation of respiratory rate can be used for approximating $F_{HF}(t)$. For the estimation of $F_{LF}(t)$, which in the AF results to be concentrated along a line, the Hough Transform (HT) is applied to $|A(\nu, \tau)|$. Due to the hermitian symmetry of the AF, HT can be performed just on $(\nu,\tau) > 0$ resulting faster than in TF domain.

The parameter $\nu_0$ in (3) is fixed imposing that $\Phi(\nu_{i,min},0;\nu_0,\tau_0,\lambda)=k<<1$ :

$$\nu_0 = \nu_{i,\min}(-\log(k)/\pi)^{-1/(4\lambda)} \qquad (5)$$

Given that no information can help to retrieve the geometry of inner ITs, which mainly oscillate in the frequency direction, to find the $\tau_0$ providing a good compromise between inner ITs suppression and TF resolution, an iterative process is proposed. The parameter $\tau_0$ is gradually reduced (increasing smoothing) until auto TF spectra are positive or, eventually $\gamma^2(t,f)$ is bounded to unity in the TF region of interest. Using the former criterion, $C_x(t,f)>0$, the inner ITs are not completely removed, but their oscillations never take negative values. Figures 1a-1b represent the case of an insufficient smoothing. Outer ITs are still present at midway between the two components and, as expected, they are higher where the two signal spectral components are closer. In Fig. 1c-1d the TF map computed with the optimized $\nu_0$ is shown. It is free from outer ITs but not from inner ones (see Fig. 1d around 0.3 Hz). Finally, in Fig. 1e-1f the $\tau_0$ for $C_x(t,f)>0$ is used.

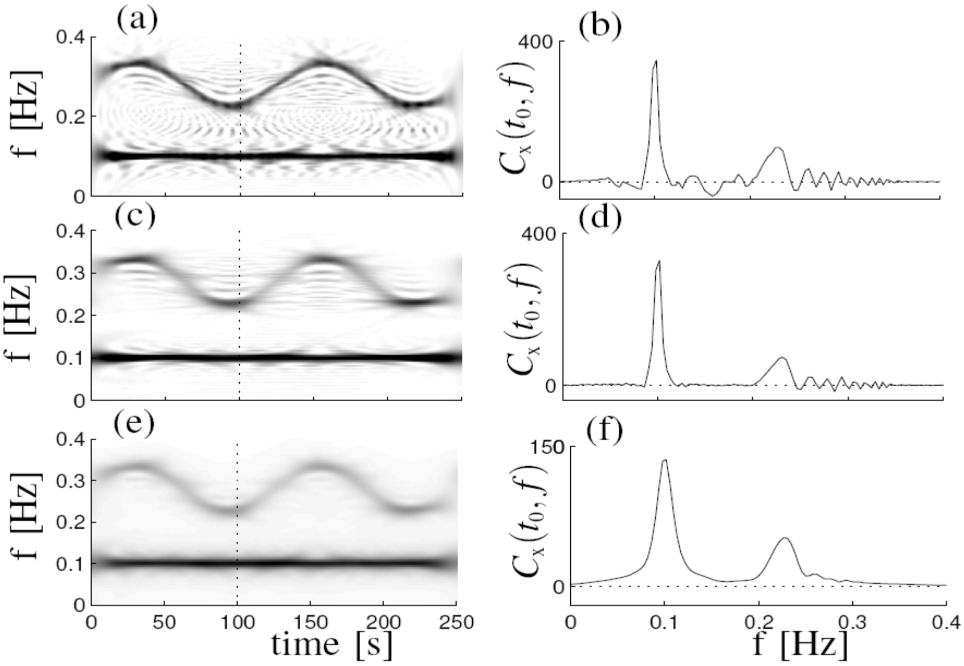


*Figure 1. Left: auto TF spectrum $C_x(t,f)$; $x(t)$ components are shown in Fig. 2 and SNR=10dB; Right: $C_x(t_0,f)$, with $t_0$ marked by a dotted line in the left panels. (a)-(b): insufficient smoothing. (c)-(d): smoothing performed with a kernel optimized for outer ITs suppression. (e)-(f): smoothing performed with a kernel optimized for both outer and inner ITs attenuation.*

### 2.3. Time-Frequency region of interest

The restriction of the TF support to a region of interest $\Omega(t,f)$ is justified by the desire of finding a good compromise between high joint TF resolution and boundness of $\gamma(t,f)$ by 1 (full suppression of ITs). The region of interest is then defined as the TF region $\Omega(t,f)$ where:

$$\forall\ t, C(t,f) > a \times \max_{f}\{C(t,f)\} \tag{6}$$

where parameter $a$<1 and $\Omega(t,f)=\Omega_x(t,f)\cap\Omega_y(t,f)$. Once that $\gamma^2(t,f)$ has been estimated, it is possible to track the time evolution of a single component coupling $\gamma^2_{LF}(t)$ and $\gamma^2_{HF}(t)$ by averaging $\gamma(t,f)$, defined in $\Omega(t,f)$, in LF and HF bands, respectively. In addition, a mean spectral coherence $\gamma(f)$ (generally different from traditional spectral coherence) is retrieved averaging TFC on time. In those rare cases when, despite the positivity of both auto spectra, for some few points $(t_0,f_0)$ $\gamma^2(t,f)$>1, the iterative process to compute $\tau_0$ continues until the number of $(t_0,f_0)$ is decreased to a very small, empirically determined, percentage of $\Omega(t,f)$ and the remaining $(t_0,f_0)$ are excluded from $(t_0,f_0)$. In this way TF resolution and the consistency of the estimator can be both preserved. Those situations are due to inner interferences, which create small oscillations in the auto spectra which are not present in the cross-spectrum.

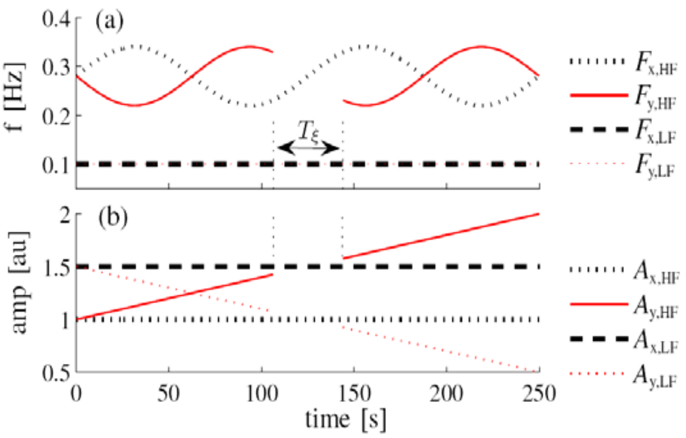


*Figure 2 Instantaneous frequencies (a) and amplitudes (b) of x(t) and y(t) used in the simulation study. In Tξ y(t) is replaced by a white noise.*

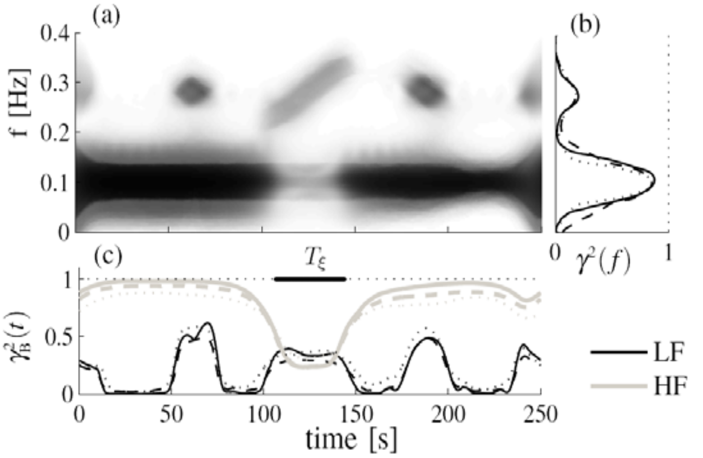


*Figure 3 (a) TFC, group average on 100 realization, between signals described in Fig. 2 when SNR=10 dB. Color map goes from 0 (white) to 1 (black). (b) $\gamma^2(f)$ is extracted from $\gamma^2(t,f)$ averaging TFC on time. (c) Band coherence $\gamma^2(t)$.*

## 3. Materials

### 3.1. Simulation study

In a simulation study the model described in (4) is used to obtain 2 deterministic signals, $x(t)$ and $y(t)$, whose instantaneous frequencies and amplitudes are shown in Fig. 2. In both cases $F_{LF}$ is constant and $F_{HF}(t)$ varies sinusoidally, which may model a situation of periodic breathing (abnormal respiration in which periods of shallow and deep breathing alternate). The amplitudes of the spectral components of $x(t)$ are constant, whereas $A_{y,LF}(t)$ and $A_{y,HF}(t)$ linearly change in time. Note that $x(t)$ and $y(t)$ are coupled in LF band whereas no coupling is present in HF band. Moreover, in order to simulate a strong decorrelating event, during the interval $T_\xi$ (see Fig. 2) $y(t)$ is replaced by a white noise with the same variance as $y(t)$. This abrupt change also introduces a very high amount of ITs in $C_y(t,f)$. One hundred pairs of signals, sampled at 4 Hz, have been created for SNR=20,10,5 dB and their TFC have been estimated.

### 3.2. Real data application

Real data application aims at exploring the linear relationship between HRV and PTTV (i.e. the time it takes a pulse wave to travel between two arterial sites) during DAP episodes related to obstructive sleep apnea (OSA). As detailed in [Gil et al.,2009], 175 selected signal segments centred on a strong DAP were extracted from complete night polysomnography recordings from 21 children (age 4.47±2.04). Pulse transit time was estimated as the interval between the peak of the R-wave on the ECG and the 50% peak value of the corresponding pulse in the finger pad measured by photoplethysmography. For every segment, the time evolution of the HRV-PTTV coupling in LF and HF band was extracted from $\gamma^2(t,f)$.

## 4. Results and discussion

### 4.1. Simulation study

Simulation results are shown in Fig. 3. The parameters $\nu_0$ and $\tau_0$ were estimated as explained above, using $\lambda$=0.25, $k$=0.002 and $a$=0.08. When the positivity of the auto spectra was not sufficient to bound $\gamma^2(t,f)$, smoothing continued until reaching a quantities of not bounded points <0.2% of $\Omega(t,f)$. Note that $\gamma^2(t,f)$ was high in LF band, except for the interval where noise replaced $y(t)$. The discontinuity introduced in $T_\xi$ was detected with a good time resolution and, as expected, correlation decreased with noise. The thinning of $\Omega(t,f)$ observed in the latest part of the simulation (see Fig. 3a) was due to the contemporary increasing of $A_{y,HF}(t)$ and decreasing of $A_{y,LF}(t)$. Given that the points $(t_0,f_0)\notin \Omega(t,f)$ are not taken into account, the change in $\Omega(t,f)$ did not affect the estimation of $\gamma^2_{LF}(t)$.

In HF, TFC was always very low, excepted when $F_{x,HF}(t)$ and $F_{y,HF}(t)$ overlapped (two gray spots around 60 and 200 s). The low but non zero values observed during $T_\xi$ in HF band were due to the fact that the TF region around $T_\xi$, $F_{x,HF}(T_\xi)\notin \Omega(t,f)$. Note that the TFC estimator performed robustly even when SNR=5dB.

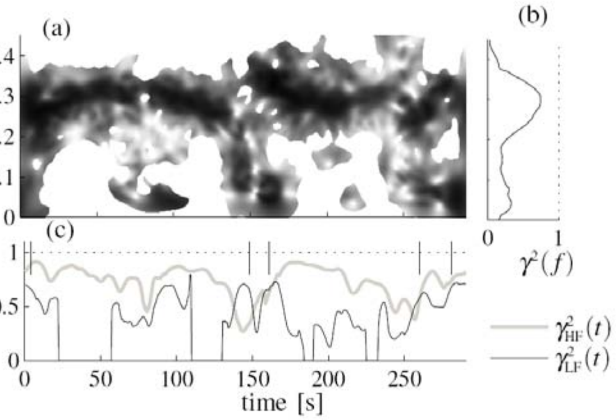


*Figure 4 (a):TFC map of one HRV-PTTV coupling. (b) $\gamma^2(f)$ is extracted from $\gamma^2(t,f)$ averaging TFC on time. (c): band coherence. vertical lines marks DAP events*

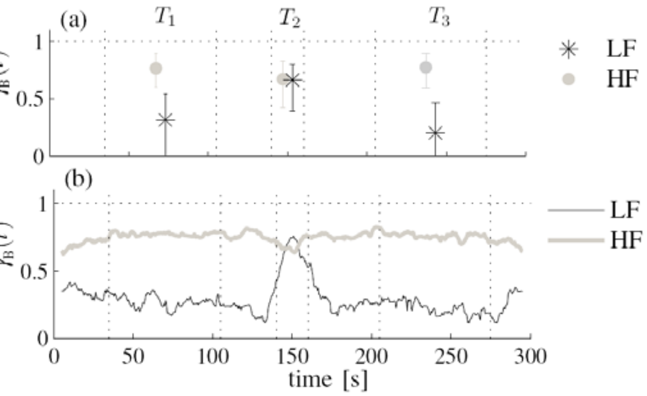


*Figure 5 (a) Interquartile range of all the median $\gamma^2(t)$ in $T_1$, $T_2$ and $T_3$. (b) Median time evolution of HRV-PTTV coupling in LF and HF range. DAP occurs in $T_2$*

### 4.2. Real data application

The TFC map of HRV-PTTV coupling in one representative signal segment is shown in Fig. 4. The white regions in the TFC map in Fig. 4a represent the TF regions which are not included in $\Omega(t,f)$, i.e. in which $\gamma^2(t,f)$ is not defined. When a DAP occurs (vertical lines) $\gamma^2_{HF}(t)$ decreased and $\gamma^2_{LF}(t)$ increased. In Fig. 5b the median trends of the 175 $\gamma^2_{HF}(t)$ *and* $\gamma^2_{HF}(t)$ are reported. The interquartile ranges of the median values of the band coherences estimated, for each signal segment, before ($T_1$), during ($T_2$) and after ($T_3$) the central DAP are plotted in Fig. 5a. Using both T-Student's test and Wilcoxon Test, the global increase of $\gamma^2_{LF}(t)$ and the global decrease of $\gamma^2_{HF}(t)$ during the central DAP resulted significant ($p$<0.05). As shown in Fig. 4, the trend of $\gamma^2(T_1)$ and $\gamma^2(T_3)$ was affected by the presence of other smaller DAPs. Analyzing separately the 26 signal segments with just one DAP, median values of $\gamma_{HF}^2(T_1)$ and $\gamma_{HF}^2(T_3)$ were observed to increase up to 0.9, while median values of $\gamma_{LF}^2(T_1)$ and $\gamma_{LF}^2(T_3)$ decreased to almost zero. Results support the idea that, in stable conditions, the respiratory component is equivalently represented in both HRV and PTTV, despite the fact that this oscillation has an autonomic origin in HRV and a mechanical one in PTTV. When a change in autonomic modulation occurs, its different origin is probably the main cause of $\gamma_{HF}^2(t)$ reduction. Concerning the LF band, it has been noticed that a sympathetic activation tends to increase the PTTV-HRV coupling. This observation may support the idea that LF in HRV can be interpreted, at least in part, as a measure of sympathetic activation.

## 5. Conclusion

In this study a framework to continuously quantify the linear coupling between cardiovascular signals using quadratic TF distributions has been presented. It represents an interesting tool for multivariate studies which aim at understanding how autonomic modulation is reflected in biomedical signals. This first application shows that in stable condition HRV and PTTV signals are highly correlated in respiratory frequency band while, during sympathetic activation, their coherence decreases in HF band and increases in LF band.

### Acknowledgements

This work was supported by CIBER de Bioingenieria, Biomateriales y Nanomedicina through ISCIII, by Project TEC-2007-68076-C02-02 from CICYT, and by Grupo Consolidado GTC from DGA (Spain)

### REFERENCES

Baraniuk and Jones DL, A signal-dependent time-frequency representation: optimal kernel design, IEEE Trans. Signal Process., vol. 41, no. 4, pp. 1589–1602, 1993.

Costa A and Boudreau-Bartels G, Design of time-frequency representations using a multiform, tiltable exponential kernel, IEEE Trans. Signal Process., vol. 43, no. 10, pp. 2283–2301, 1995.

Gil E, Mendez M, Vergara JM, Cerutti S, Bianchi AM, and Laguna P, Discrimination of sleep apnea related decreases in the amplitude fluctuations of ppg signal in children by HRV analysis, IEEE Trans. Biomed. Eng., vol. 56, n. 4, pp. *1005-1014, 2009*

Hlawatsch F, Duality and classification of bilinear time-frequency signal representations, IEEE Trans. Signal Process., vol. 39, no. 7, pp. 1564–1574, 1991

Hlawatsch F, Flandrin P, The Wigner Distribution -theory and applications in signal processing. Elsevier, pp. 59–113, 1997

Keissar K, Davrath LR, and Akselrod S, Coherence analysis between respiration and heart rate variability using continuous wavelet transform, Phil. Trans. R. Soc. A, vol. 367, no. 1892, pp. 1393–1406, 2009.

Mainardi LT and al., Multivariate time-variant identification of cardiovascular variability signals: a beat-to-beat spectral parameter estimation in vasovagal syncope, IEEE Trans. Biomed. Eng., vol. 44, no. 10, pp. 978–989, 1997.

Mainardi LT, On the quantification of heart rate variability spectral parameters using time-frequency and time-varying methods, Phil. Trans. R. Soc. A, vol. 367, no. 1887, pp. 255–275, 2009.

Matz G and Hlawatsch F, Time-frequency coherence analysis of nonstationary random processes, in Proc. Tenth IEEE Workshop on Statistical Signal and Array Processing, pp. 554–558, 2000

Orini M, Bailón R, Laguna P, and Mainardi LT, Modeling and estimation of time-varying heart rate variability during stress test by parametric and non parametric analysis, in Proc. Computers in Cardiology, pp. 29–32, 2007

Porta A and al., Quantifying the strength of the linear causal coupling in closed loop interacting cardiovascular variability signals, Biol Cybern, vol. 86, no. 3, pp. 241–251, 2002.

Porta A, Baselli G, and Cerutti S, Implicit and explicit model-based signal processing for the analysis of short-term cardiovascular interactions, Proceedings of the IEEE, vol. 94, no. 4, pp. 805–818, 2006.

White LB and Boashash B, Cross spectral analysis of nonstationary processes, IEEE Trans. Inf. Theory, vol. 36, no. 4, pp. 830–835, 1990

Zhao H, Cupples WA, Ju KH, and Chon KH, Time-varying causal coherence function and its application to renal blood pressure and blood flow data, IEEE Trans. Biomed. Eng., vol. 54, no. 12, pp. 2142–2150, 2007.

.

.